HEPATOLOGY
Official Journal of the American Association for the Study of Liver Diseases

Modeling Correction of Severe Urea Cycle Defects in the Growing Murine Liver Using a Hybrid Recombinant Adeno-Associated Virus/*piggyBac* Transposase Gene Delivery System

Sharon C. Cunningham,[1,2] Susan M. Siew,[1] Claus V. Hallwirth,[1] Christine Bolitho,[1] Natsuki Sasaki,[1] Gagan Garg,[1,3] Iacovos P. Michael,[4] Nicola A. Hetherington,[1] Kevin Carpenter,[5] Gustavo de Alencastro,[1] Andras Nagy,[4,6,7] and Ian E. Alexander[1,8]

Liver-targeted gene therapy based on recombinant adeno-associated viral vectors (rAAV) shows promising therapeutic efficacy in animal models and adult-focused clinical trials. This promise, however, is not directly translatable to the growing liver, where high rates of hepatocellular proliferation are accompanied by loss of episomal rAAV genomes and subsequently a loss in therapeutic efficacy. We have developed a hybrid rAAV/*piggyBac* transposon vector system combining the highly efficient liver-targeting properties of rAAV with stable *piggyBac*-mediated transposition of the transgene into the hepatocyte genome. Transposition efficiency was first tested using an enhanced green fluorescent protein expression cassette following delivery to newborn wild-type mice, with a 20-fold increase in stably gene-modified hepatocytes observed 4 weeks posttreatment compared to traditional rAAV gene delivery. We next modeled the therapeutic potential of the system in the context of severe urea cycle defects. A single treatment in the perinatal period was sufficient to confer robust and stable phenotype correction in the ornithine transcarbamylase–deficient *Spf*^{ash} mouse and the neonatal lethal argininosuccinate synthetase knockout mouse. Finally, transposon integration patterns were analyzed, revealing 127,386 unique integration sites which conformed to previously published *piggyBac* data. *Conclusion:* Using a hybrid rAAV/*piggyBac* transposon vector system, we achieved stable therapeutic protection in two urea cycle defect mouse models; a clinically conceivable early application of this technology in the management of severe urea cycle defects could be as a bridging therapy while awaiting liver transplantation; further improvement of the system will result from the development of highly human liver-tropic capsids, the use of alternative strategies to achieve transient transposase expression, and engineered refinements in the safety profile of *piggyBac* transposase-mediated integration. (HEPATOLOGY 2015;62:417-428)

Severe urea cycle defects (UCDs) presenting in the newborn period with hyperammonemia are associated with high morbidity and mortality if not recognized early and managed aggressively.[1] Acute control of hyperammonemia, which is highly neurotoxic, requires intensive care intervention, such as venovenous hemofiltration, accompanied by alternative pathway therapy, stringent dietary protein restriction, supplementation with urea cycle intermediates, and strict avoidance of catabolism.[2] Long-term survival with quality of life necessitates liver transplantation, and prevention of recurrent episodes of hyperammonemia while awaiting transplantation is often difficult to achieve. Liver-targeted gene therapy is therefore an

Abbreviations: AAV2, adeno-associated virus 2 genome; ASS, argininosuccinate synthetase; cDNA, complementary DNA; EGFP, enhanced green fluorescent protein; FIX, factor IX; IS, integration site; LSP1, liver-specific promoter 1; MRC, matched random control; mRNA, messenger RNA; OTC, ornithine transcarbamylase; pAAV2, plasmid AAV2; PB, piggyBac *transposase; PCR, polymerase chain reaction; rAAV, recombinant adeno-associated virus; SB, Sleeping Beauty; shRNA, short hairpin RNA; Spf*^{ash}*, sparse fur abnormal skin and hair; TIR, piggyBac transposon terminal inverted repeat; TSS, transcription start site; UCD, urea cycle defect.*

attractive prospect, with exciting therapeutic promise recently reported for factor IX (FIX) deficiency in the adult liver using vectors based on recombinant adeno-associated virus (rAAV).[3,4] This promise, however, is not directly translatable to the growing liver, where high rates of hepatocellular proliferation are accompanied by loss of episomal rAAV genomes.[5,6]

Toward addressing this challenge, we have developed a hybrid rAAV/*piggyBac* transposon vector system combining the highly efficient liver-targeting properties of rAAV with stable *piggyBac*-mediated transposition of the expression cassette into the hepatocyte genome. The *piggyBac* transposon system, isolated from the cabbage looper moth (*Trichopulsia ni*),[7] was selected for evaluation based on a number of theoretical advantages over *Tc1/mariner*-type transposons, such as *Sleeping Beauty* (SB). These include greater activity in a diversity of mammalian cell types,[8,9] no reduction in the efficiency of transposition up to and beyond the packaging capacity of AAV vectors,[8] and seamless excision,[10] such that reexcision events occurring while transposase expression persists do not mutagenize the host cell genome.

The impetus of our study was to achieve stabilized gene expression in the developing liver, where we and others have previously shown rapid clearance of rAAV episomal genomes in concert with hepatocellular proliferation. This phenomenon has been further shown to underpin progressive loss of therapeutic efficacy, initially achieved in the neonatal period, in mouse models of UCDs[11,12] where relatively high levels of stable gene transfer are required to achieve phenotype correction. We therefore chose to model the therapeutic potential of this system in the challenging context of UCDs. A single treatment with the hybrid system in the perinatal period was sufficient to confer robust and stable phenotype correction in the partially ornithine transcarbamylase (OTC)–deficient *Spf*^{ash} (sparse fur abnormal skin and hair) mouse and the neonatal lethal argininosuccinate synthetase (ASS) knockout mouse. Histological and molecular analyses revealed unprecedented levels of stable gene transfer, which were maintained into adulthood.

Materials and Methods

AAV Vector Construction and Production. The coding sequence of *piggyBac* transposase was amplified by polymerase chain reaction (PCR) from pCAG- *piggyBac* transposase (PB)[13] and inserted into the plasmid adeno-associated virus 2 genome (pAAV2)-liver specific promoter 1 (LSP1).enhanced green fluorescent protein (EGFP),[6] replacing the EGFP coding sequence to produce pAAV2-LSP1.PB. The 5′ (313 bp) and 3′ (230 bp) *piggyBac* transposon terminal inverted repeats (TIRs) were amplified by PCR from pPB-CA-GFP[14] and inserted into pAAV2-LSP1.EGFP, immediately internal to AAV2 inverted terminal repeats and flanking the transgene cassette. The resulting vector construct was designated pAAV2-LSP1.EGFP-TIR. To produce the therapeutic transposon vector constructs pAAV2-LSP1.mOTC-TIR and pAAV2-LSP1.mASS-TIR, the EGFP complementary DNA (cDNA) in pAAV2-LSP1.EGFP-TIR was replaced with the cDNA for either murine OTC (NM 008769.3) or ASS (NM 007494). To produce the EGFP transposon vector construct with shortened *piggyBac* TIRs, pAAV2-LP1.EGFP-TIR(sh), the minimal TIRs (67 bp, 40 bp)[15] were PCR-amplified and exchanged for the longer TIRs in pAAV2-LSP1.EGFP-TIR. The vector constructs for knockdown of endogenous OTC messenger RNA (mRNA; pAAV2-LSP1.EGFP-H1.OTCshort

From the [1]Gene Therapy Research Unit, Children's Medical Research Institute and The Children's Hospital at Westmead, Westmead, New South Wales, Australia; [2]University of Sydney Medical School, Sydney, New South Wales, Australia; [3]Department of Chemistry and Biomolecular Sciences, Macquarie University, Macquarie Park, New South Wales, Australia; [4]Lunenfeld-Tanenbaum Research Institute, Mount Sinai Hospital, Toronto, Ontario, Canada; [5]Biochemical Genetics, The Children's Hospital at Westmead, Westmead, Sydney, New South Wales, Australia; [6]Institute of Medical Science and Department of Obstetrics & Gynaecology, University of Toronto, Toronto, Ontario, Canada; [7]Department of Obstetrics & Gynaecology, University of Toronto, Toronto, Ontario, Canada; [8]Discipline of Paediatrics and Child Health, The University of Sydney, Sydney, New South Wales, Australia

Received January 28, 2015; accepted April 7, 2015.

Additional Supporting Information may be found at http://onlinelibrary.wiley.com/doi/10.1002/hep.27842/suppinfo

Supported by National Health and Medical Research Council project grants (APP1065053 and APP1026710, to S.C.C. and C.V.H.) and by grants from the Ontario Research Fund Global Leadership Round in Genomics and Life Sciences and the Canadian Institutes of Health Research (CIHR MOP102575, to A.N., a tier 1 Canada Research Chair in Stem Cells and Regeneration).

Address reprint requests to: Professor Ian E. Alexander, Head, Gene Therapy Research Unit, Children's Medical Research Institute, 214 Hawkesbury Road, Westmead, NSW, Australia 2145. E-mail: ian.alexander@health.nsw.gov.au; tel: +61-2-98453031; fax: +61-2-98451317.

View this article online at wileyonlinelibrary.com.

DOI 10.1002/hep.27842

Potential conflict of interest: Nothing to report.

hairpin RNA [shRNA] or nonspecific) were produced as described.[16]

Recombinant AAV vectors were produced in HEK 293 cells[17] pseudo-serotyped with the AAV8 or AAVrh10 capsid as described.[6] Vector genome titers were assigned by real-time quantitative PCR targeting the woodchuck postregulatory element sequence[16] or the EGFP transgene (see below, Vector Copy Number Analysis).

Cell Culture. HEK 293 cells were cultured in Dulbecco's modified Eagle medium (Gibco, Invitrogen, Grand Island, NY) supplemented with 10% (v/v) fetal bovine serum (JRH Biosciences, Lenexa, KS) and 1% (w/v) L-glutamine (Gibco, Invitrogen) and maintained at 37°C in a humidified 5% CO_2–air atmosphere.

Animal Procedures. Breeding pairs of *Spf*^{ash} mice (B6EiC3Sn *a/A-Otc*$^{spf\text{-}ash}$/J; stock no. 001811) and ASS-deficient mice (B6;129S7-*Ass1*^{tm1Bay}/J; stock no. 002189) were purchased from the Jackson Laboratory (Bar Harbor, ME). Animals were housed in a temperature-controlled environment on a 12-hour light/dark cycle with water and standard rodent chow (18.9% [wt/wt] protein; Specialty Feeds, Glen Forrest, Australia) supplied *ad libitum*. All experimental procedures were evaluated and approved by the institutional Animal Care and Ethics Committee. Vector administration to newborn and adult mice was by intraperitoneal injection in volumes of 20 μL and 100 μL, respectively. For *in utero* injection of vector at E15, pregnant females were anesthetized and a laparotomy was performed to expose the uterus. Each fetus was injected intraabdominally with 5 μL of vector through the uterine wall. The abdominal incision was sutured closed, and mice were subjected to a regime of ampicillin and carprofen until parturition (designated day 0).

Blood and Urine Biochemistry. Blood was collected either by tail vein nick or by cardiac puncture (terminal procedure) into lithium heparin-coated tubes and centrifuged at 7500*g* for 5 minutes at 4°C. Plasma was frozen in liquid nitrogen and stored at −80°C. For amino acid quantitation, plasma was analyzed by ion-exchange chromatography.[12] Plasma ammonia was measured using the Ammonia Assay Kit (catalog no. AA0100; Sigma-Aldrich, St Louis, MO). For urinary orotic acid analysis, urine was collected over a 24-hour period on Whatman filter paper, eluted, and measured using liquid chromatography/tandem mass spectrometry.[12]

Fluorometry. Fluorometric analysis was used to quantitate EGFP in liver lysate as described.[18]

OTC Enzyme Activity Assay. Liver lysate OTC activity and distribution across the hepatic lobule in frozen liver sections were determined as described.[19]

14C-Radiochemical Assay for ASS Enzyme Activity. The ASS activity in the liver was determined based on the conversion of ^{14}C-aspartate to ^{14}C-argininosuccinate[20] with minor modifications.[12]

Immunofluorescence and Immunohistochemistry. For detection of EGFP, livers were removed and fixed in 4% (wt/v) paraformaldehyde in phosphate-buffered saline, cryoprotected in 10%-30% (wt/v) sucrose, and frozen in optimum cutting temperature (TissueTek; Sakura Finetek, Torrance, CA) in isopentane/liquid nitrogen. For colocalization of gene-modified cells with specific regions of liver architecture, central veins were identified by immunohistochemical staining of glutamine synthetase. Frozen sections (5 μm) were permeabilized in methanol, then reacted with a rabbit anti–glutamine synthetase primary antibody (1/150 dilution; catalog no. ab16802; Abcam, Cambridge, UK). Bound primary antibody was detected with an Alexa Fluor 594 donkey antirabbit secondary antibody (1/1000 dilution; catalog no. A21207; Invitrogen, Carlsbad, CA). Sections were mounted in Immu-Mount (Thermo-Shandon) and imaged using an Olympus (Center Valley, PA) BX51 fluorescent microscope. Direct EGFP fluorescence was detected using filters D480/30× (excitation) and D535/40m (emission), and Alexa Fluor 594 was detected using filters HQ560/55 (excitation) and HQ645/75 (emission). The percentage of transduced cells was determined by counting EGFP-positive cells in three random fields of view (10× magnification).

For localization of ASS protein, livers were removed and fixed in neutral-buffered formalin. Antigen retrieval using 10 mmol/L sodium citrate buffer (pH 7.4) was followed by blocking with 0.3% (v/v) hydrogen peroxidase for 30 minutes. Endogenous avidin and biotin were blocked using an avidin-biotin kit (catalog no. SP2001; Vector Laboratories, Burlingame, CA). After blocking with 10% (v/v) donkey serum, sections were incubated with a goat antimouse ASS primary antibody (2.5 μg/mL; catalog no. ab77590; Abcam), followed by a biotinylated donkey antigoat secondary antibody (1.2 μg/mL, catalog no. 705-065-147; Jackson ImmunoResearch, West Grove, PA). Sections were reacted with the Vectastain Elite ABC system (PK-7100; Vector Laboratories) and 3,3′-diaminobenzidine liquid substrate (catalog no. D6190; Sigma-Aldrich). To identify the central veins, a rabbit anti–glutamine synthetase primary antibody (as above) was used. Bound primary antibody was detected with a biotinylated donkey antirabbit secondary antibody (1/1000; catalog no. 711-065-152; Jackson ImmunoResearch) and the Vectastain Elite ABC system, followed by VIP substrate (catalog no. SK-4600; Vector Laboratories).

Sections were counterstained with hematoxylin, mounted with Ultramount No. 4 (Fronine), and imaged using a Zeiss Axio Imager.A1 microscope and Spot Imaging software.

Vector Copy Number Analysis. Liver DNA was extracted using standard phenol/chloroform and ethanol precipitation methods,[21] and vector genome copy numbers were determined by real-time quantitative PCR. The vector copy number of the transposon rAAVs was determined using the Quantitect Sybr Green Kit (Qiagen, Valencia, CA) and the following oligonucleotide sets: EGFP-F/EGFP-R, OTC-F/OTC-R, and ASS-F/ASS-R. Vector copy number of the *piggyBac* transposase rAAV was determined using the Takara Sybr Premix Ex Taq Kit (catalog no. RR420A) and oligonucleotides PB-F/PB-R. The PCRs were normalized using the Quantitect Sybr Green Kit and the oligonucleotide set glyceraldehyde 3-phosphate dehydrogenase F/R. All oligonucleotide sequences are described in Supporting Table S1. Each reaction contained 100-150 ng of genomic DNA. Standards were prepared from linearized plasmid, diluted in a background of 100-150 ng human genomic liver DNA per reaction.

mRNA Expression. Total RNA was extracted from 30-50 mg liver tissue using Trizol reagent (catalog no. 15596018; Life Technologies) and treated with DNAse I (catalog no. 18068015; Life Technologies). Reverse transcription using the SuperScript III First-Strand Synthesis SuperMix (catalog no. 18080400; Life Technologies) was used to generate cDNA. Quantitative real-time PCR was performed using the Quantitect Sybr Green Kit and the relevant oligonucleotide sets (Supporting Table S1).

Integration Site Recovery. Total DNA was extracted from 60 mg of liver tissue using the High Pure PCR Template Preparation Kit (catalog no. 11796828001; Roche) according to the manufacturer's protocol with the following modifications. Liver tissue was digested in Proteinase K for 3 hours, and following extraction, the samples underwent an additional RNAse A treatment (catalog no. 158924; Qiagen) and DNA purification by organic extraction and ethanol precipitation. The DNA (20 μg) was digested overnight with MluCI (catalog no. R0538L; NEB) and purified by organic extraction and ethanol precipitation. The 5' overhangs were partially filled in with Klenow Fragment (3'→5' exo-) (catalog no. M0212L; NEB). Oligonucleotides A and B (Supporting Table S1) were annealed and ligated to the DNA fragments using T4 DNA ligase (catalog no. M0202L; NEB). The ligation products were purified by organic extraction and ethanol precipitation. Ligation-mediated PCRs were performed with 250 ng DNA template per 50-μL reaction, using HotStarTaq *Plus* DNA polymerase (catalog no. 203603; Qiagen) at a final $MgCl_2$ concentration of 2 mM and a mixture of oligonucleotides C, D, and E under the following cycling conditions: once at 95°C for 5 minutes, seven times at 94°C for 30 seconds and at 72°C for 1 minute, 37 times at 94°C for 30 seconds and at 68°C for 1 minute, and once at 68°C for 3 minutes. Oligonucleotides C and D (Supporting Table S1) primed amplification from either end of the integrated *piggyBac* sequence, while oligonucleotide E primed from the ligated linkers. Aliquots (3 μL) from each amplification reaction were pooled and separated on a 2.5% (w/v) agarose gel. Amplicons (150-600 bp) were extracted using a Wizard SV Gel and PCR Clean-Up System (catalog no. A9282; Promega). The fragment library was sequenced on an IlluminaMiSeq platform (Australian Genome Research Facility) with 40% phi X174 control library spike-in, using an R1 primer mix comprising the standard Illumina R1 primer and custom sequencing oligonucleotides F and G and an R2 primer mix comprising the standard Illumina R2 primer and custom sequencing oligonucleotide H.

Integration Site Analysis. IlluminaMiSeq reads were processed by trimming distal (where present) and proximal adapter sequences using Bowtie[22] and custom Perl scripts (available on request). Trimmed reads were mapped as pairs to the mouse reference genome mm9 using Bowtie. Matched random control (MRC) sites were generated by retaining all TTAA sequences that conformed to the experimental conditions of integration site (IS) retrieval in terms of proximity to MluCI recognition sequences. Classification of ISs as transcription start site (TSS)-proximal, intragenic, and intergenic was made relative to the University of California Santa Cruz known gene TSSs using BEDtools.[23] For the statistical analysis of IS counts relative to MRCs, sites were counted in intervals of TSS ± 100 kb at all coding gene loci annotated in mm9. Numerical IS and MRC counts for all intervals were individually compared using two-tailed Fisher's exact test to obtain *P* values. Representation values relative to MRCs were obtained for each coding gene by expressing interval counts as frequencies with respect to the size of the *piggyBac* IS or the MRC data set and then dividing the IS frequency by the MRC frequency for every interval.

Hair Microscopy. Strands of hair from a wild-type and a treated mutant mouse were mounted in

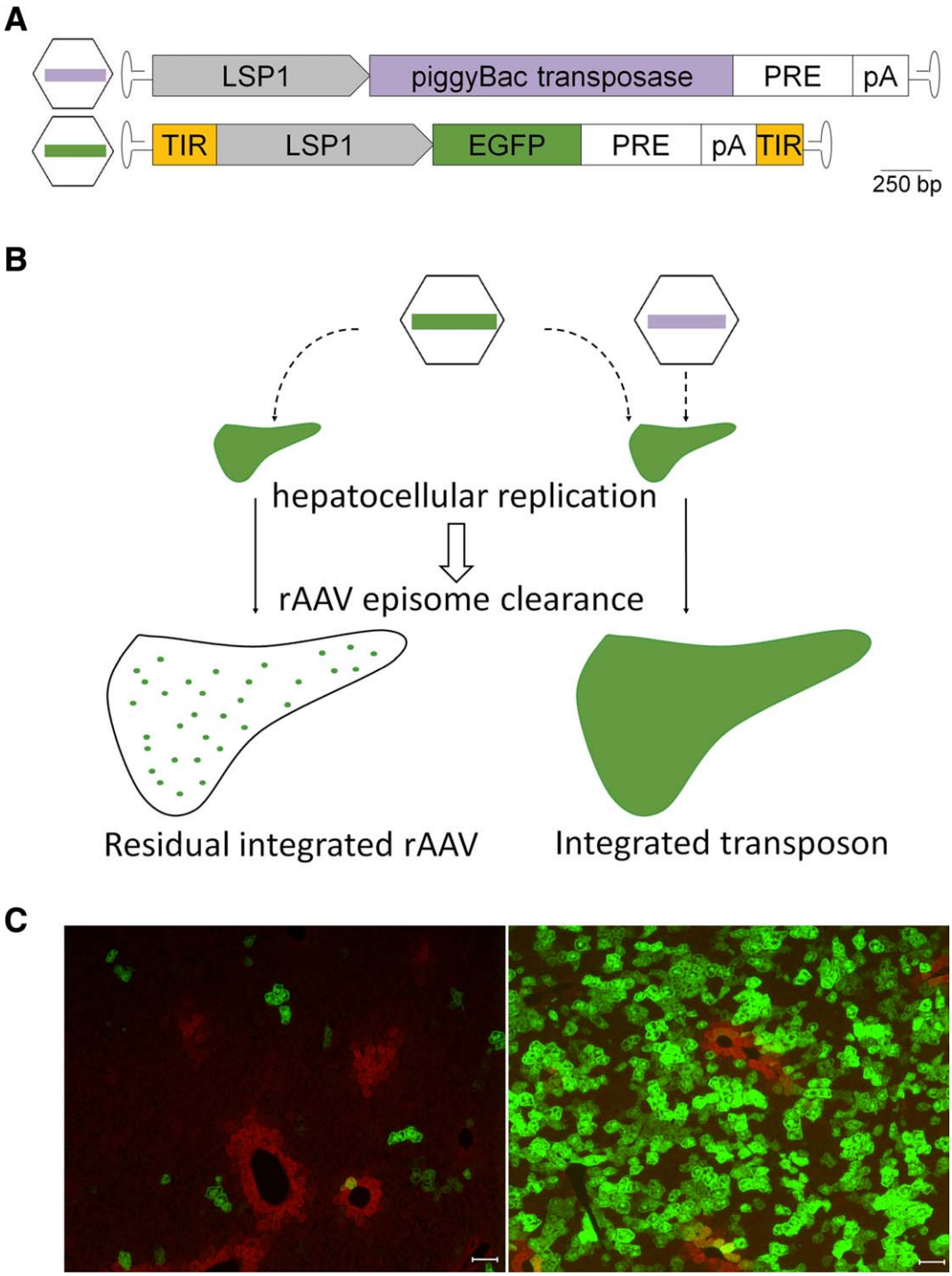

Fig. 1. Hybrid rAAV/*piggyBac* deployment strategy for stable transduction of the newborn mouse liver. (A) Schematic representation of AAV vector constructs encoding *piggyBac* transposase (top) or a transposable EGFP expression cassette (bottom). Hairpin structures represent AAV inverted terminal repeats. (B) Mechanism of action. (C) Representative histological sections from mouse livers harvested at 4 weeks of age after transduction in the newborn period (1-2 days) with the transposon-encoding AAV2/8 vector alone (left) at a dose of 1×10^{11} vector genomes per mouse (n = 4) or in combination with the *piggyBac* transposase-encoding AAV2/8 vector (right) at a dose of 5×10^{10} vector genomes per mouse (n = 4). Green fluorescence indicates EGFP expression, and red indicates endogenous glutamine synthetase expression (central vein marker). Scale bar = 50 μm. Abbreviations: PRE, posttranscriptional regulatory element; pA, bovine growth hormone polyadenylation signal.

Immu-Mount on a microscope slide and imaged using a Zeiss Axio Imager.A1 microscope and Spot Imaging software.

Statistics. The nonparametric Mann-Whitney *U* test was applied to all data sets as normal distribution was not assumed due to small sample size. Results

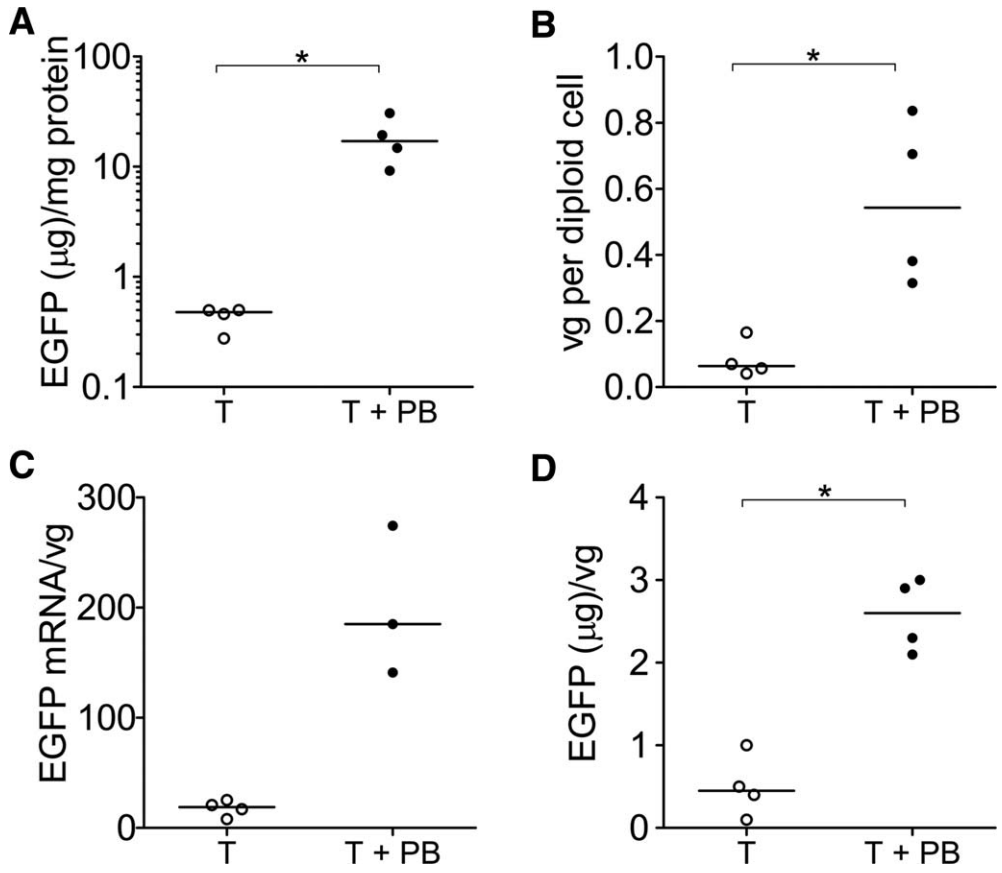

Fig. 2. Molecular analyses on transduced liver expressing EGFP. (A) Fluorometric quantitation of EGFP expression in liver lysates. (B) Vector genome copy number per diploid liver cell. (C,D) Relative EGPF mRNA and protein expression per vector genome copy number (arbitrary units). Dot plots show median values. EGFP transposon-encoding vector alone (T) or in combination with the *piggyBac* transposase-encoding vector (T+PB) are indicated by open and closed dots, respectively. For statistical comparison of experimental groups, the nonparametric Mann-Whitney *U* test was used (*$P < 0.05$). Significance tests were not performed where sample size was n = 3. Abbreviation: vg, vector genome.

were analyzed using GraphPad Prism (GraphPad Software, La Jolla, CA) and presented as scatterplots to show variation, with median values indicated. *P* values ≤ 0.05 were considered statistically significant.

Results

Stable Transduction of the Newborn Mouse Liver Using the Hybrid rAAV/piggyBac System. In configuring our prototype hybrid rAAV/*piggyBac* vector system we used a two-virion approach[24,25] by placing *piggyBac* transposase under the control of a hepatocyte-specific promoter in one AAV construct and *piggyBac* TIRs flanking the transgene expression cassette in a second transposon donor AAV construct (Fig. 1A). These rAAV2/TIR constructs were pseudoserotyped with the highly murine liver-tropic AAV8 capsid to produce vector stocks capable of achieving efficient two-hit kinetics in the mouse liver. By deploying the system in the growing liver, we strategically exploited the loss of rAAV episomes that occurs in concert with hepatocellular proliferation to achieve transient *piggyBac* transposase expression in the vast majority of transduced hepatocytes (Fig. 1B). This limits ongoing loss of successfully transposed expression cassettes by cycles of genomic insertion and reexcision.

The system was initially tested in wild-type mice using an EGFP reporter gene. The AAV vector containing an EGFP expression cassette embedded in a *piggyBac* transposon was delivered to newborn pups, with and without codelivery of the vector encoding the *piggyBac* transposase. Histological analysis of liver (Fig. 1C) at 4 weeks of age, after rAAV episome clearance,[6] demonstrated a >20-fold increase in the number of stably gene-modified hepatocytes from 2.4% to 50% with codelivery of the transposase expression vector. Interestingly, this correlated with a 43-fold higher level of EGFP protein expression in liver lysates (Fig. 2A), and a relatively lower, but nevertheless impressive, seven-fold increase in vector copy number per diploid cell (Fig. 2B). This indicates significantly higher levels of EGFP mRNA (Fig. 2C) and protein (Fig. 2D)

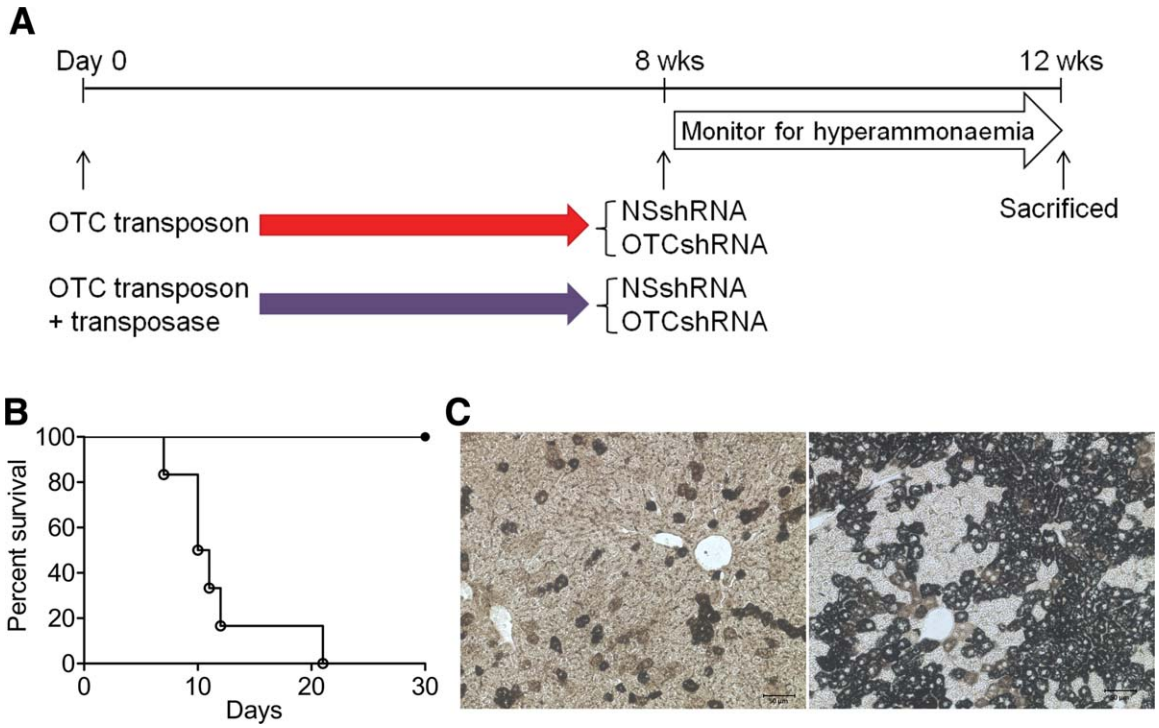

Fig. 3. Phenotype correction following gene delivery to the newborn OTC-deficient *Spf*^{ash} mouse. (A) Experimental protocol. Male *Spf*^{ash} mice were treated as newborns (1-2 days) with OTC transposon-encoding AAV2/8 vector alone, at a dose of 1×10^{11} vector genomes per mouse (n = 12), or in combination with the *piggyBac* transposase-encoding AAV2/8 vector, at a dose of 5×10^{10} vector genomes per mouse (n = 12). Upon reaching adulthood (8-10 weeks), mice in each treatment group were injected with an AAV2/rh10 knockdown vector expressing either shRNA, designed to target endogenous murine OTC mRNA (n = 6), or negative control shRNA (nonspecific, n = 6; data not shown). Mice were killed upon development of signs of hyperammonemia (ataxia, tremors, and lethargy) or 1 month later, whichever came first. (B) Kaplan-Meier survival analysis of treated *Spf*^{ash} mice following knockdown of endogenous residual OTC activity. Open dots indicate treatment with OTC transposon-encoding AAV2/8 vector alone (n = 6), while closed dots indicate treatment with both the OTC transposon-encoding AAV2/8 vector and the *piggyBac* transposase-encoding AAV2/8 vector (n = 6). (C) Representative histological sections from mouse livers transduced with either OTC transposon-encoding vector alone (left) or in combination with the *piggyBac* transposase encoding vector (right). Cells expressing OTC activity stain brown with an intensity that correlates with the level of enzymatic activity. Scale bar = 100 μm. Abbreviation: NS, nonspecific.

expression from transposed expression cassettes than from those stably maintained (presumably through integration) in the host cell as part of an AAV provirus.

Given the limited packaging capacity of AAV vectors, we next sought to increase the cargo capacity of the vector-encoded transposable element by evaluating the efficacy of the system using minimal *piggyBac* TIRs[15] (Supporting Fig. S1). Quantitatively and qualitatively equivalent data were obtained (Supporting Fig. S2). The hybrid system performed similarly in male and female mice, delivering impressive 70-fold and 103-fold increases in stable EGFP expression at 3 and 8 weeks of age, respectively, over the transposon vector delivered alone. The perivenous and periportal zones of the hepatic lobule, which exhibit metabolic zonation,[26] were targeted with equivalent efficiency (Supporting Fig. S2A).

Stable Phenotype Correction in Mouse Models of Severe UCDs. Using the partially OTC-deficient *Spf*^{ash} mouse, we have previously shown that the maximum level of stable gene transfer achievable following rAAV-mediated treatment of newborn mice (~8% of hepatocytes) is insufficient to prevent shRNA-induced lethal hyperammonemia in adulthood when background endogenous OTC activity (5%-7%) is knocked down (<3%) following rAAV delivery of an shRNA specific for endogenous OTC mRNA.[16] The equivalent experiment was repeated using the hybrid rAAV/*piggyBac* system modified to express the murine OTC cDNA (Fig. 3A; Supporting Fig. S1). Mice treated with the rAAV OTC transposon alone developed severe hyperammonemia, necessitating euthanasia, when background endogenous OTC activity was knocked down, while mice treated with both the OTC-expressing transposon and transposase-encoding vectors survived (Fig. 3B), as did all cohorts injected with a negative control rAAV expressing a nonspecific shRNA (data not shown). This correlated with an approximately 66-fold increase in the proportion of visibly OTC-positive hepatocytes in liver sections (Fig.

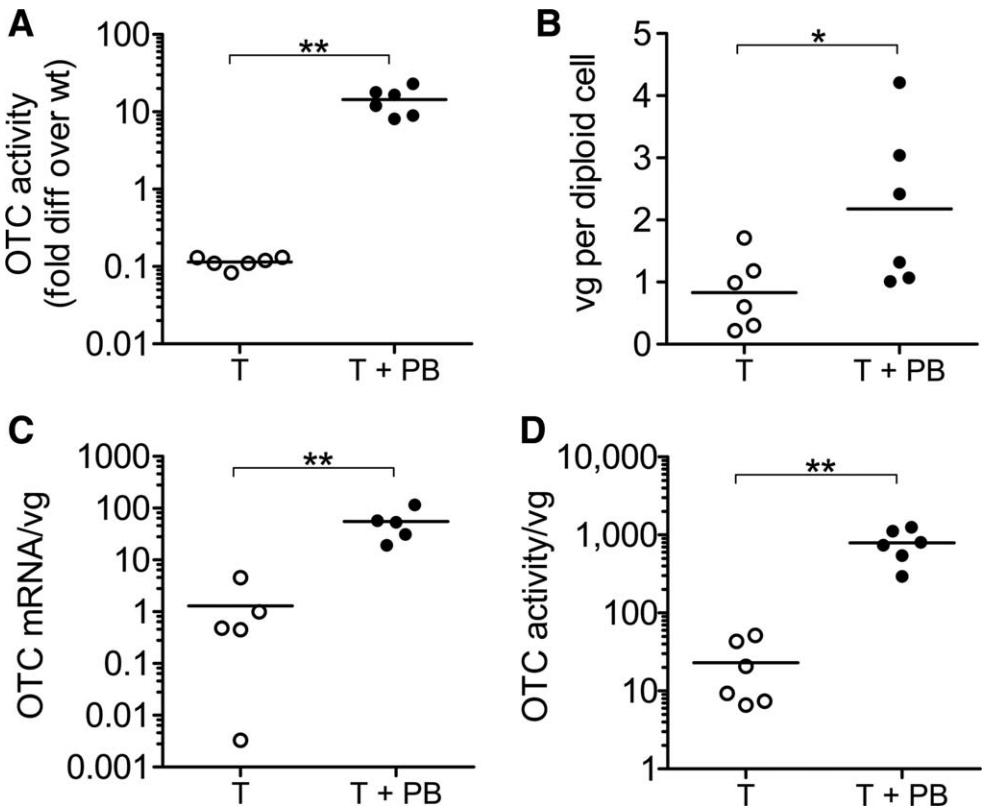

Fig. 4. Molecular analyses on liver from treated *Spf*^{ash} mice. (A) Liver lysate OTC enzymatic activity as a percentage of wild type. (B) Quantitation of vector genome copy number per diploid liver cell. (C,D) Relative murine OTC mRNA and protein expression per vector genome copy number (arbitrary units). Dot plots show median values. Open and closed dots, respectively, indicate OTC transposon-encoding vector alone and in combination with the *piggyBac* transposase-encoding vector. For statistical comparison of experimental groups, the nonparametric Mann-Whitney *U* test was used (*$P < 0.05$, **$P < 0.01$). Abbreviation: vg, vector genome.

3C) and a 126-fold increase in OTC activity to massively supraphysiological levels (Fig. 4A). Consistent with data generated using the EGFP-encoding constructs, the increase in stably maintained vector genome copies was less dramatic (Fig. 4B), again indicating higher levels of transgene expression from transposed expression cassettes (Figs. 4C,D).

We next evaluated the hybrid rAAV/*piggyBac* system in the neonatal lethal citrullinemic (ASS knockout) mouse, which more directly recapitulates the clinical presentation of infants with severe UCDs and is characterized by severe hyperammonemia, elevated plasma citrulline, reduced plasma arginine, and elevated urinary orotic acid.[27,28] In an earlier study we reported successful rescue of neonatal lethality using conventional rAAV, but survival into adulthood required vector redelivery during liver growth to maintain therapeutic levels of ASS expression.[12] In contrast, using the hybrid rAAV/*piggyBac* system encoding the murine ASS cDNA under essentially the same experimental conditions (Fig. 5A), we show that following a single prenatal dose mutant mice not only survived the neonatal period but remained healthy into adulthood, with one cohort maintained to 6 months of age. Rescued mutant males and females were fertile, and females carried pups to full term. A sparse fur, abnormal skin and hair phenotype was evident from birth, reminiscent of that observed in juvenile OTC-deficient *Spf*^{ash} mice, which improved from weaning age (Fig. 5B,C). Histological analysis confirmed similarly high levels of stable gene transfer to those obtained with EGFP and OTC transgenes (Fig. 5D). Most importantly, all treated mice exhibited robust control of hyperammonemia, the clinically relevant metabolic disturbance, despite intermouse variability in ASS activity (Fig. 6A). More sensitive measures of urea cycle function, including plasma citrulline (Fig. 6B), plasma arginine (Fig. 6C), and urinary orotate levels (Fig. 6D), revealed a residual metabolic phenotype.

Analysis of piggyBac ISs. In a preliminary safety assessment, integration patterns were analyzed in mouse liver following delivery of the hybrid rAAV/*piggyBac* system in the newborn period. We mapped 127,386 unique *piggyBac* ISs (Supporting Table S2) and, in the absence of *in vivo* data sets of equivalent complexity, compared these to published data sets in

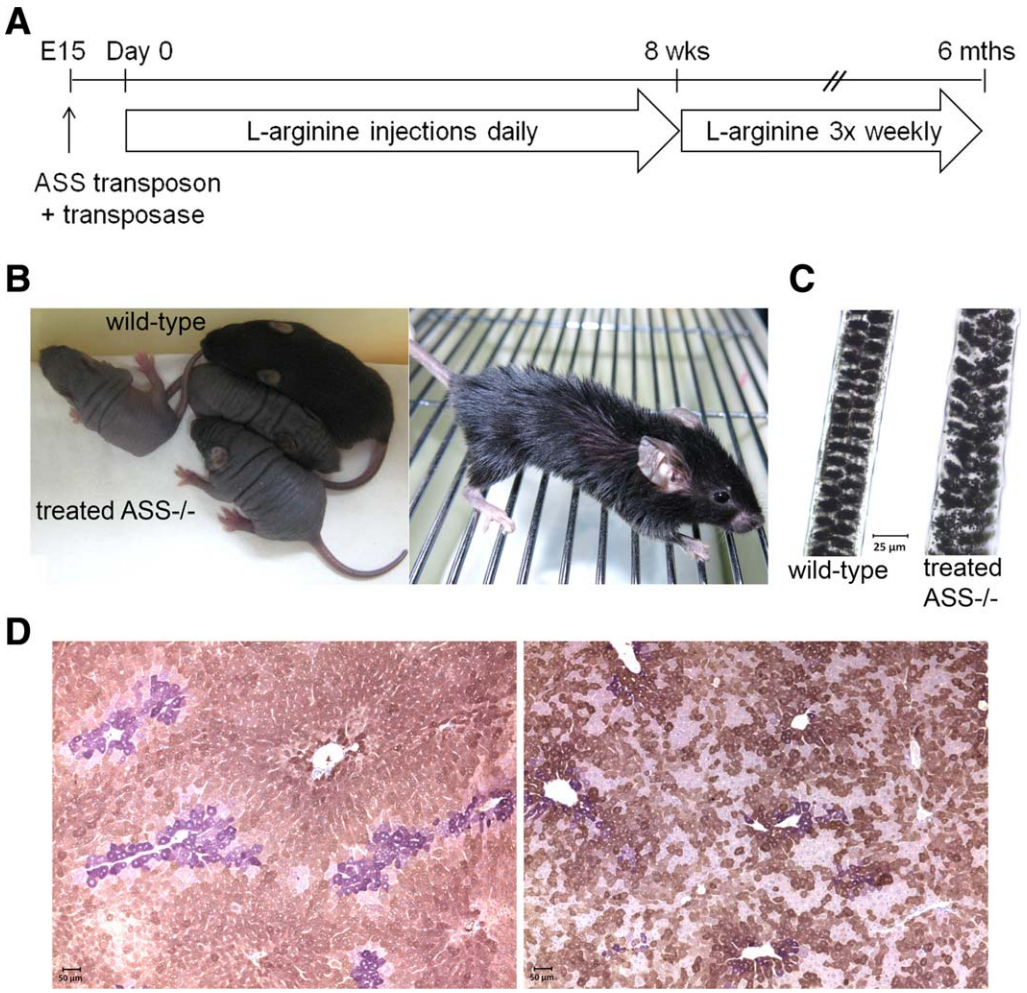

Fig. 5. Phenotype correction in a neonatal lethal mouse model of ASS deficiency following a single dose *in utero*. (A) Experimental protocol. Time-matched heterozygous breeding pairs were established to generate homozygous offspring. At embryonic day 15, the gravid uterus was externalized and each fetus was injected with the ASS transposon rAAV (1×10^{11} vector genome) in combination with the *piggyBac* transposase rAAV (5×10^{10} vector genome) in a total volume of 5 μL. From birth, pups were given a daily intraperitoneal injection of L-arginine (1 g/kg) until adulthood, after which injections were reduced to three times weekly. Mice were monitored and sacrificed from 3 to 6 months of age. (B) Treated mutant pups and wild-type littermates at 10 days of age (left panel) and treated mutant adult mouse (right panel). (C) Microscopic analysis of hair strands from a wild-type and treated adult mutant ($Ass^{-/-}$) mouse. Scale bar = 25 μm. (D) Representative histological images from a wild-type control liver (left) and a treated mutant mouse liver (right). Brown staining indicates the presence of ASS protein by antibody detection, while purple staining indicates glutamine synthetase. Scale bar = 50 μm.

mouse cells. The IS distributions conformed to published *piggyBac* data in terms of preferential integration in the proximity of TSSs, albeit to a lesser extent than for γ-retroviral vectors (Fig. 7). Furthermore, *piggyBac* integrations in intragenic regions were less frequent compared to lentiviral vectors. The complexity of the IS data set facilitated statistical analysis of integration frequencies at known protein-coding genes in the mouse genome (Supporting Fig. S3 and Table S3). While the degree of overrepresentation at individual loci correlated only weakly with expression levels (data not shown), the most significantly and highly overrepresented genes are associated with liver function, in particular Afp and Alb (Supporting Fig. S3), which is consistent with observations by others following AAV integration in the neonatal liver.[29] Importantly, genes implicated as drivers of hepatocellular carcinoma[30] were not among these, nor was integration overrepresented at the *Rian-Mirg* locus linked to AAV integration–induced hepatocellular carcinoma[29,31,32] (Supporting Fig. S4).

Transient Expression of piggyBac Transposase. As stated earlier, deployment of the hybrid rAAV/transposase system in the growing liver was predicted to achieve transient transposase expression in the majority of hepatocytes (>90%) through the loss of rAAV episomes that accompanies hepatocellular proliferation (Fig. 1B). Vector copy number analysis confirmed this hypothesis, with *piggyBac* transposase detected in the

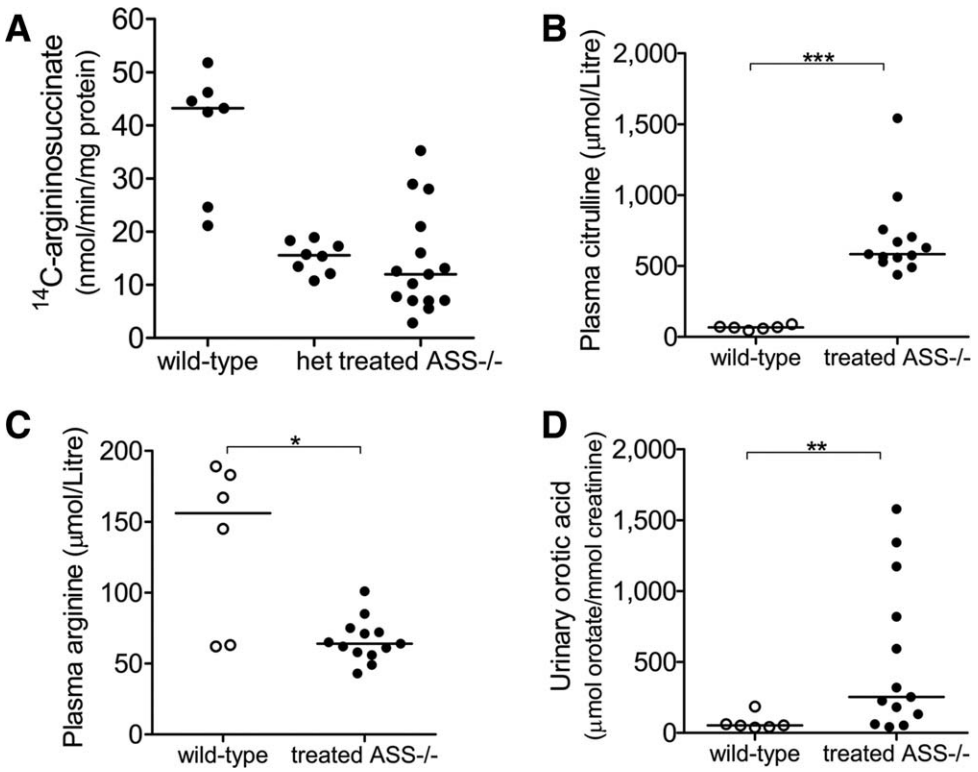

Fig. 6. Enzymatic and biochemical analyses on liver and plasma from treated citrullinemic mice. (A) Liver lysate ASS enzyme activity from wild-type and heterozygous (het) males and females and treated mutant ($Ass^{-/-}$) adult mice, determined by quantifying the level of conversion of ^{14}C-aspartate to ^{14}C-argininosuccinate. Plasma citrulline (B), plasma arginine (C), and urinary orotic acid (D) in control (wild-type) mice (open symbols) and treated mutant adult ($Ass^{-/-}$) mice (closed symbols). Dot plots show median values. For statistical comparison of experimental groups, the nonparametric Mann-Whitney *U* test was used (*$P < 0.1$, **$P < 0.01$, ***$P < 0.001$).

equivalent of 7% of cells at the completion of each experiment (0.07 ± 0.02 vector copies per diploid cell).

Discussion

Highly efficient and stable gene transfer to the growing liver has not been previously possible. In the present study, using a novel liver-targeted rAAV/*piggyBac* transposase system, we show that a single treatment in the perinatal period is sufficient to confer robust and stable control of hyperammonemia into adulthood in murine models of two therapeutically challenging UCDs: OTC and ASS deficiency. As is seen following liver transplantation for both OTC and ASS deficiency, plasma levels of the urea cycle intermediates citrulline and arginine were not completely normalized.[33-35] This reflects the persistence of extrahepatic deficiency of urea cycle enzymes, rather than insufficient liver-targeted gene transfer, and is readily managed clinically by oral arginine supplementation.

Hybrid viral vector/transposon systems have been described exploiting native and hyperactive forms of SB transposase, in the context of both adenovirus and AAV-mediated gene transfer[24,25]; and more recently similar reports using *piggybac*-mediated transposition have begun to appear.[36] To date, however, only systems based on adenovirus in combination with SB transposition have been evaluated in the liver, with FIX expression used to model therapeutic potential.[24,37] Stable therapeutic levels of FIX ($\geq$1% physiological) have been achieved in mice and a canine model, but molecular data correlating the underlying proportion of hepatocytes stably modified by transposition are limited to a single dog. In this animal, with FIX levels close to 1% of physiological values, a maximal estimate of transposon integration frequency was 0.01 copies per cell.[37] Recently reported *in vitro* data generated using a hybrid rAAV/SB transposon vector system showed similarly low levels of stable transposition in cultured HeLa cells, even when optimally configured with the hyperactive SB100X transposase.[25] Plausible explanations for the dramatically improved performance of the hybrid delivery system reported here include the use of the *piggyBac* transposon system, the use of a highly hepatotropic AAV vector pseudo-

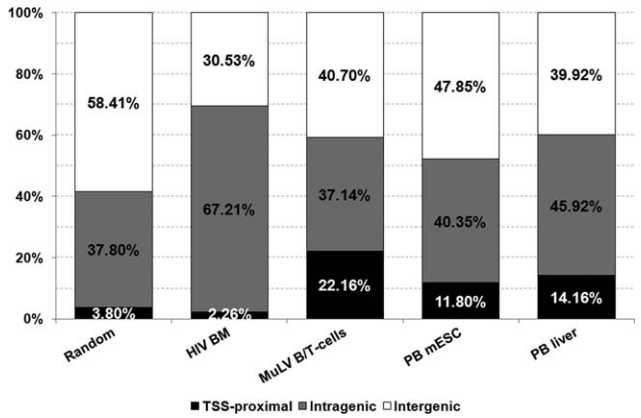

Fig. 7. Analysis of *piggyBac* integration patterns in mouse liver. Comparison of integration profiles relative to University of California Santa Cruz known genes (http://genome.ucsc.edu/). Categorization of ISs was defined according to published definitions[45]: TSS-proximal sites are located within 2.5 kb upstream or downstream of a TSS; intragenic sites are located between the TSS and the transcription end site (except for those sites that fulfill the criterion of being TSS-proximal); and all remaining sites are regarded as intergenic. The data sets consist of the following: Random, 200,000 TTAA sites matched to the experimental conditions of IS recovery in this study; HIV BM, 796 ISs recovered from pretransplantation bone marrow cells transduced with a lentiviral vector in a β-thalassemia study[46]; MuLV B/T-cells, 12,951 singleton γ-retroviral vector ISs[47,48] from B/T-cell tumors; PB mESC, 131,594 *piggyBac* ISs recovered without drug selection[49]; PB liver, 127,386 *piggyBac* ISs recovered from liver taken from a 4-week-old mouse injected in the newborn period with EGFP transposon/PB transposase rAAV in this study. *P* values (Fisher's exact test) of specific comparisons referred to in the main text: TSS-proximal MuLV versus *piggyBac* integrations $= 7.8 \times 10^{-119}$; intragenic HIV versus *piggyBac* integrations $= 1.9 \times 10^{-33}$.

serotype, and a deployment strategy in the developing liver ensuring transient transposase expression in the vast majority of hepatocytes.

An interesting observation made with each set of experiments was that significantly higher levels of mRNA and protein expression resulted from transposed expression cassettes than from stably maintained (presumably through integration) AAV provirus. Vector genome integration, possibly in the form of concatemers,[38] may be accompanied by vector genome rearrangement, deletions, and insertions.[38-40] All of these alterations may affect transgene expression.

The major unresolved consideration for possible future human use of the hybrid rAAV/*piggyBac* system is safety, given the inherent oncogenic risk of integrating gene transfer systems.[41-43] In ongoing studies, a cohort of six mice, injected as newborns with OTC transposon/*piggyBac* transposase rAAVs, has been maintained beyond 12 months with continuing observation. Furthermore, vector integration profile comparisons of *piggyBac* (in mouse liver) with other integrating vector systems (Fig. 7) indicate a reduced proclivity toward TSS-proximal integration relative to γ-retroviral vectors. This translates to a comparatively lower risk of insertional activation of proto-oncogenes. Moreover, a lower propensity for intragenic integration relative to lentiviral vectors reduces the risk for disruption of gene function.

The potential of this hybrid AAV/*piggyBac* system for clinical use will increase with ongoing advances in AAV-based gene delivery technology, particularly the development of highly human liver-tropic capsids,[44] the use of alternative strategies to achieve transient transposase expression such as mRNA-mediated delivery, and engineered refinements in the safety profile of *piggyBac* transposase–mediated integration. Because there remains a risk of insertional mutagenesis, a clinically conceivable early application of this technology in the management of severe UCDs could be as a bridging therapy while awaiting liver transplantation.

References

1. Batshaw ML, Tuchman M, Summar M, Seminara J; Members of the Urea Cycle Disorders Consortium. A longitudinal study of urea cycle disorders. Mol Genet Metab 2014;113:127-130.
2. Haberle J, Boddaert N, Burlina A, Chakrapani A, Dixon M, Huemer M, et al. Suggested guidelines for the diagnosis and management of urea cycle disorders. Orphanet J Rare Dis 2012;7:32.
3. Nathwani AC, Tuddenham EG, Rangarajan S, Rosales C, McIntosh J, Linch DC, et al. Adenovirus-associated virus vector-mediated gene transfer in hemophilia B. N Engl J Med 2011;365:2357-2365.
4. Nathwani AC, Reiss UM, Tuddenham EGD, Rosales C, Chowdary P, McIntosh J, et al. Long-term safety and efficacy of factor IX gene therapy in haemophilia B. N Engl J Med 2014;371:1994-2004.
5. **Wang Z**, **Zhu T**, Qiao C, Zhou L, Wang B, Zhang J, et al. Adeno-associated virus serotype 8 efficiently delivers genes to muscle and heart. Nat Biotechnol 2005;23:321-328.
6. Cunningham SC, Dane AP, Spinoulas A, Alexander IE. Gene delivery to the juvenile mouse liver using AAV2/8 vectors. Mol Ther 2008;16:1081-1088.
7. Fraser MJ, Ciszczon T, Elick T, Bauser C. Precise excision of TTAA-specific lepidopteran transposons piggyBac (IFP2) and tagalong (TFP3) from the baculovirus genome in cell lines from two species of Lepidoptera. Insect Mol Biol 1996;5:141-151.
8. **Ding S**, **Wu X**, Li G, Han M, Zhuang Y, Xu T. Efficient transposition of the piggyBac (PB) transposon in mammalian cells and mice. Cell 2005;122:473-483.
9. Wu SC, Meir YJ, Coates CJ, Handler AM, Pelczar P, Moisyadi S, et al. piggyBac is a flexible and highly active transposon as compared to sleeping beauty, Tol2, and Mos1 in mammalian cells. Proc Natl Acad Sci USA 2006;103:15008-15013.
10. Elick TA, Bauser CA, Fraser MJ. Excision of the piggyBac transposable element in vitro is a precise event that is enhanced by the expression of its encoded transposase. Genetica 1996;98:33-41.
11. Cunningham SC, Spinoulas A, Carpenter KH, Wilcken B, Kuchel PW, Alexander IE. AAV2/8-mediated correction of OTC deficiency is robust in adult but not neonatal *Spf*^{ash} mice. Mol Ther 2009;17:1340-1346.
12. Kok CY, Cunningham SC, Carpenter KH, Dane AP, Siew SM, Logan GJ, et al. Adeno-associated virus-mediated rescue of neonatal lethality in argininosuccinate synthetase deficient mice. Mol Ther 2013;21:1823-1831.
13. Wang W, Lin C, Lu D, Ning Z, Cox T, Melvin D, et al. Chromosomal transposition of PiggyBac in mouse embryonic stem cells. Proc Natl Acad Sci USA 2008;105:9290-9295.

14. Woltjen K, Hamalainen R, Kibschull M, Mileikovsky M, Nagy A. Transgene-free production of pluripotent stem cells using piggyBac transposons. Methods Mol Biol 2011;767:87-103.
15. Meir YJ, Weirauch MT, Yang HS, Chung PC, Yu RK, Wu SC. Genome-wide target profiling of piggyBac and Tol2 in HEK 293: pros and cons for gene discovery and gene therapy. BMC Biotechnol 2011;11:28.
16. Cunningham SC, Kok CY, Dane AP, Carpenter K, Kizana E, Kuchel PW, et al. Induction and prevention of severe hyperammonemia in the spfash mouse model of ornithine transcarbamylase deficiency using shRNA and rAAV-mediated gene delivery. Mol Ther 2011;19:854-859.
17. Graham FL, Smiley J, Russell WC, Nairn R. Characteristics of a human cell line transformed by DNA from human adenovirus type 5. J Gen Virol 1977;36:59-74.
18. Dane AP, Wowro SJ, Cunningham SC, Alexander IE. Comparison of gene transfer to the murine liver following intraperitoneal and intraportal delivery of hepatotropic AAV pseudo-serotypes. Gene Ther 2013; 20:460-464.
19. Ye X, Robinson MB, Batshaw ML, Furth EE, Smith I, Wilson JM. Prolonged metabolic correction in adult ornithine transcarbamylase-deficient mice with adenoviral vectors. J Biol Chem 1996;271:3639-3646.
20. Ye X, Whiteman B, Jerebtsova M, Batshaw ML. Correction of argininosuccinate synthetase (AS) deficiency in a murine model of citrullinemia with recombinant adenovirus carrying human AS cDNA. Gene Ther 2000;7:1777-1782.
21. Sambrook J, Fritsch EF, Maniatis T. Molecular Cloning: A Laboratory Manual. Cold Spring Harbor, NY: Cold Spring Harbor Laboratory Press, 1989.
22. Langmead B, Trapnell C, Pop M, Salzberg SL. Ultrafast and memory-efficient alignment of short DNA sequences to the human genome. Genome Biol 2009;10:R25.21-R25.10.
23. Quinlan AR, Hall IM. BEDTools: a flexible suite of utilities for comparing genomic features. Bioinformatics 2010;26:841-842.
24. Yant SR, Ehrhardt A, Mikkelsen JG, Meuse L, Pham T, Kay MA. Transposition from a gutless adeno-transposon vector stabilizes transgene expression in vivo. Nat Biotechnol 2002;20:999-1005.
25. Zhang W, Solanki M, Muther N, Ebel M, Wang J, Sun C, et al. Hybrid adeno-associated viral vectors utilizing transposase-mediated somatic integration for stable transgene expression in human cells. PLoS One 2013;8:e76771.
26. Jungermann K, Katz N. Functional specialization of different hepatocyte populations. Physiol Rev 1989;69:708-764.
27. Patejunas G, Bradley A, Beaudet AL, O'Brien WE. Generation of a mouse model for citrullinemia by targeted disruption of the argininosuccinate synthetase gene. Somat Cell Mol Genet 1994;20:55-60.
28. Deignan JL, Cederbaum SD, Grody WW. Contrasting features of urea cycle disorders in human patients and knockout mouse models. Mol Genet Metab 2008;93:7-14.
29. Chandler RJ, LaFave MC, Varshney GK, Trivedi NS, Carrillo-Carrasco N, Senac JS, et al. Vector design influences hepatic genotoxicity after adeno-associated virus gene therapy. J Clin Invest 2015;125: 870-880.
30. Woo HG, Park ES, Lee JS, Lee YH, Ishikawa T, Kim YJ, et al. Identification of potential driver genes in human liver carcinoma by genome-wide screening. Cancer Res 2009;69:4059-4066.
31. **Donsante A**, **Miller DG**, Li Y, Vogler C, Brunt EM, Russell DW, et al. AAV vector integration sites in mouse hepatocellular carcinoma. Science 2007;317:477.
32. **Wang PR**, **Xu M**, Toffanin S, Li Y, Llovet JM, Russell DW. Induction of hepatocellular carcinoma by in vivo gene targeting. Proc Natl Acad Sci USA 2012;109:11264-11269.
33. Rabier D, Narcy C, Bardet J, Parvy P, Saudubray JM, Kamoun P. Arginine remains an essential amino acid after liver transplantation in urea cycle enzyme deficiencies. J Inherit Metab Dis 1991;14:277-280.
34. Kawamoto S, Strong RW, Kerlin P, Lynch SV, Steadman C, Kobayashi K, et al. Orthotopic liver transplantation for adult-onset type II citrullinaemia. Clin Transplant 1997;11:453-458.
35. Ban K, Sugiyama N, Sugiyama K, Wada Y, Suzuki T, Hashimoto T, et al. A pediatric patient with classical citrullinemia who underwent living-related partial liver transplantation. Transplantation 2001;71:1495-1497.
36. Cooney AL, Singh B, Sinn PL. Hybrid nonviral/viral vector systems for improved piggyBac DNA transposon in vivo delivery. Mol Ther 2015; 23:667-674.
37. Hausl MA, Zhang W, Muther N, Rauschhuber C, Franck HG, Merricks EP, et al. Hyperactive sleeping beauty transposase enables persistent phenotypic correction in mice and a canine model for hemophilia B. Mol Ther 2010;18:1896-1906.
38. Deyle DR, Russell DW. Adeno-associated virus vector integration. Curr Opin Mol Ther 2009;11:442-447.
39. Nakai H, Wu X, Fuess S, Storm TA, Munroe D, Montini E, et al. Large-scale molecular characterization of adeno-associated virus vector integration in mouse liver. J Virol 2005;79:3606-3614.
40. Miller DG, Petek LM, Russell DW. Adeno-associated virus vectors integrate at chromosome breakage sites. Nat Genet 2004;36:767-773.
41. Cavazza A, Moiani A, Mavilio F. Mechanisms of retroviral integration and mutagenesis. Hum Gene Ther 2013;24:119-131.
42. Hacein-Bey-Abina S, von Kalle C, Schmidt M, Le Deist F, Wulffraat N, McIntyre E, et al. A serious adverse event after successful gene therapy for X-linked severe combined immunodeficiency. N Engl J Med 2003;348:255-256.
43. **Stein S**, **Ott MG**, Schultze-Strasser S, Jauch A, Burwinkel B, Kinner A, et al. Genomic instability and myelodysplasia with monosomy 7 consequent to EVI1 activation after gene therapy for chronic granulomatous disease. Nat Med 2010;16:198-204.
44. Lisowski L, Dane AP, Chu K, Zhang Y, Cunningham SC, Wilson EM, et al. Selection and evaluation of clinically relevant AAV variants in a xenograft liver model. Nature 2014;506:382-286.
45. Cattoglio C, Pellin D, Rizzi E, Maruggi G, Corti G, Miselli F, et al. High-definition mapping of retroviral integration sites identifies active regulatory elements in human multipotent hematopoietic progenitors. Blood 2010;116:5507-5517.
46. Ronen K, Negre O, Roth S, Colomb C, Malani N, Denaro M, et al. Distribution of lentiviral vector integration sites in mice following therapeutic gene transfer to treat beta-thalassemia. Mol Ther 2011;19:1273-1286.
47. **Uren AG**, **Kool J**, Matentzoglu K, de Ridder J, Mattison J, van Uitert M, et al. Large-scale mutagenesis in p19(ARF)- and p53-deficient mice identifies cancer genes and their collaborative networks. Cell 2008;133:727-741.
48. Kool J, Uren AG, Martins CP, Sie D, de Ridder J, Turner G, et al. Insertional mutagenesis in mice deficient for p15Ink4b, p16Ink4a, p21Cip1, and p27Kip1 reveals cancer gene interactions and correlations with tumor phenotypes. Cancer Res 2010;70:520-531.
49. **de Jong J**, **Akhtar W**, Badhai J, Rust AG, Rad R, Hilkens J, et al. Chromatin landscapes of retroviral and transposon integration profiles. PLoS Genet 2014;10:e1004250.

Author names in bold designate shared co-first authorship.

Supporting Information

Additional Supporting Information may be found at http://onlinelibrary.wiley.com/doi/10.1002/hep.27842/suppinfo.